Journal of Science and Engineering Technology, Vol. 4, No. 4, pp. 71-77 (2008)

Optical Properties of Chiral Photonic Crystals Containing Birefringent Microstructural Forms

JIUN-YEU CHEN[1], JIA-YI YEH[2], CHIN-TIEN LIN[3] and MING-YING HSU[4]

[1]*Center for General Education, Hsing Kuo University of Management*

600, Sec. 3, Taijing Blvd., Annan District, Tainan, Taiwan 709, R.O.C.

[2]*Department of Management Information Science, Chung Hwa University of Medical Technology*

89, Wen-Hwa lst St., Jen-Te Hsiang, Tainan Hsien, Taiwan 717, R.O.C.

[3]*Department of Information Science, Hsing Kuo University of Management*

600, Sec. 3, Taijing Blvd., Annan District, Tainan, Taiwan 709, R.O.C.

[4]*Instrument Technology Research Center, National Applied Research Laboratories*

20 R&D Rd. VI, Hsinchu Science Park, Hsinchu, Taiwan 300, R.O.C.

ABSTRACT

Photonic localization in a chiral photonic structure with defective high-spatial-frequency gratings was investigated by using the finite element method. The form-birefringence effect, caused by grating high-spatial frequency, is introduced into the chiral structure by modifying the grating parameters, such as groove depth, filling factor, and refractive index of the intermixing material. This defect gives rise to a peak in transmission for circularly-polarized light having the same handedness as the helical structure. The artificial dielectrics, caused by the form-birefringence effect, play a fundamental role in restraining and manipulating light to affect the location, power transmittance and phase retardation of the defect mode. By changing the intermixing material of the grating into a different medium, the linearity of the sweep in a defective wavelength depends on the refractive index of the medium. This procedure can be applied to real photonic devices. For example, an optical refractometer or a (bio-)chemical sensor can be designed by replacing the intermixing material by the medium to be measured.

***Key Words*:** form-birefringence, chiral photonic structure, defect mode, high-spatial-frequency grating

具形狀雙折射微結構之手徵光子晶體的光學特性

陳俊宇[1]　葉佳益[2]　林金田[3]　徐名瑩[4]

[1]興國管理學院通識中心

709 台南市安南區台江大道 600 號

[2]中華醫事科技大學資訊管理系

717 臺南縣仁德鄉文華一街 89 號

[3]興國管理學院資訊科學系

709 台南市安南區台江大道 600 號

[4]國家實驗研究院儀器科技研究中心

300 新竹市科學園區研發 6 路 20 號

摘 要

本文利用有限元素法分析以高空間頻率光柵作爲手徵光子晶體缺陷的光子局域化現象。透過修改光柵參數，如溝槽深度、填充因子和混合材料的折射率，把高空間頻率光柵所產生的形狀雙折射效應引入手徵結構，而這樣的缺陷對於和螺旋結構有相同手性的圓偏振光會產生穿透度上的峰值。由形狀雙折射效應所產生的人造介電材料，在光的限制和操控上會扮演十分重要的角色，會影響缺陷模態的位置，能量穿透度以及相位延遲。而改變與光柵相互搭配的介質，缺陷波長會隨著介質折射率的變化產生線性的改變。這種具有光柵結構的手徵性光子系統能夠提供另一種可能性的方法來建構實際的光子裝置，例如生物/化學感測器或折射率計。

關鍵詞：形狀雙折射，手徵光子結構，缺陷模態，高空間頻率光柵

I. INTRODUCTION

Photonic crystals (PCs) that have an ordered structure with a modulation of refractive index or dielectric constant have attracted considerable attention from both fundamental and practical points of views. The main characteristic of PCs is that they have photonic band-gaps (PBGs) for photons, which is analogous with the electronic band structures for electrons in semiconductors [6]. In addition, the phenomenon of light localization in defect modes with discrete frequencies lying in the PBGs can be used for narrowband filtering and low-threshold lasing [4, 14]. By using the PBGs or the defect modes, light emission and propagation can be controlled arbitrarily, and realization of various new optical components is expected [11]. Among many PBG materials, chiral PCs with helical structures are very attractive. They can be synthesized by an appropriate chemical mixture to self-assemble such as cholesteric liquid crystals (CLCs) and ferroelectric liquid crystals [15, 16], or can be constructed by physical vapor deposition such as sculptured thin films [10]. In the planar texture of CLCs, the selective reflection band for circularly polarized light in the direction of structural anisotropy is created by coherent multiple scattering on distributed circular Bragg reflection structures. A circularly polarized light with the same handedness as the cholesterics propagating along a helical axis is forbidden. Light of opposite chirality is unaffected by the structure [2].

Furthermore, a rich variety of defects introduced into the perfect chiral structure have been proposed [20, 21]. A defect can be created by inserting an optically isotropic/anisotropic layer in CLCs. By the discontinuity in the helix, a twist defect results in the localized modes at the position of the defect. Based on numerical analyses, an alternative method to generate photonic defect modes is the modulation of helical twisting power [13]. In a hybrid system consisting of CLC films with different pitches but same screws, the defect modes appear at the band edge of the sandwiched CLC layer [17]. A similar structure consisting of three CLC films, the middle of which has the opposite handedness helix to either side, was found that the defect states appear when the defect mode coincides with the edge mode [22]. Quasi-periodic Fibonaccian phase defects introduced into single-pitched CLC systems can result in the optical features of simultaneous red, green, and blue reflections or multiple PBGs [3]. Defect modes in chiral PCs have received much attention and may be used for narrow band filters, low threshold lasers, and display applications.

In the use of subwavelength structures, a high-spatial-frequency grating (HSFG) has interesting optical properties. Such a grating produces no diffracted orders and reveals form birefringence. One can create artificial dielectric materials that have an effective index of refraction or other optical features that do not exist normally in nature [23]. A common difficulty associated with diffraction based components is the dependence of the diffraction angle upon the incident wavelength. In the case of zero-order gratings, only one transmitted and one reflected orders exist. The zero diffraction order is transmitted without wavelength dependence and a change in the direction of propagation, and the light of higher diffraction orders becomes evanescent. Thus, the grating behaves like a homogeneous material. To adjust the effective optical properties, one only needs to adjust the amount of intermixing between the substrate and incident material. The ability to control a region's effective index of refraction is an advantage that effective mediums have over standard optical-thin films. Such gratings have been used to produce beam splitters, wave plates, antireflection layers, and form birefringence [1, 18, 24].

The aim of this study was to explore whether the introduction of a HSFG has any utility and what limitations originate in chiral PCs. The model is based on a multilayer structure produced by a HSFG layer and two CLC films. Localized refractive perturbations within the anisotropic periodic index profile of CLCs will modify the wave

interference effects. The control of defect mode wavelengths is investigated theoretically, and the defect modes related to the grating configuration are studied to understand the effects of variable filling factor, groove depth, and the composition of the two materials with different refractive indices. To calculating the electromagnetic wave transmission and reflection in this structure, the numerical treatment is based on the three-dimensional finite element method (3D FEM) [5]. By making optical measurements of defect modes resulting from the birefringence formation, one can obtain the intermixing between the sample and the subwavelength structure. For potential applications, the hybrid system can serve as a (bio-)chemical sensor or an optical refractometer.

II. SIMULATION MODEL

To produce photonic defect modes, one way is to add an optically isotropic defect layer in the middle of a CLC as shown in Fig. 1(a) [20]. Another way to create a defect by a twist defect in the cholesteric helix or the combination of twist defect and defect layer is not considered here [20]. Fig. 1(b) shows the hybrid system, which is a multilayer structure containing a grating layer sandwiched by two identical CLC films. In Fig. 1(c), the semi-infinite geometry configuration with periodic boundary conditions in the x- and y-directions is modeled to treat the HSFG diffraction problem. The absorbing boundary condition is applied at the two ends (input and output) in the FEM model to truncate the finite element mesh in the scattering problems. For the rectangular grating layer shown in Fig. 1(d), when the grating periodicity Λ is much smaller than the wavelength λ, the binary profile with refractive indices n_1 and n_2 results in form birefringence effect (effective refractive indices $n_{eff,e}$ and $n_{eff,o}$) [1]. Through the grating equation, single-beam behavior is possible for normal incidence to require that

$$\Lambda \le \lambda/n_1,\ \Lambda \le \lambda/n_2. \tag{1}$$

Because of the geometric anisotropy of the grating structure, two orthogonally polarized waves, parallel and perpendicular to the grating grooves, suffer different effective dielectric constants and thus obtain a phase delay between them. The grating behaves like a negative uniaxial crystal. The effective refractive indices for extraordinary and ordinary beams can be estimated from second-order effective medium theory (EMT) [19]:

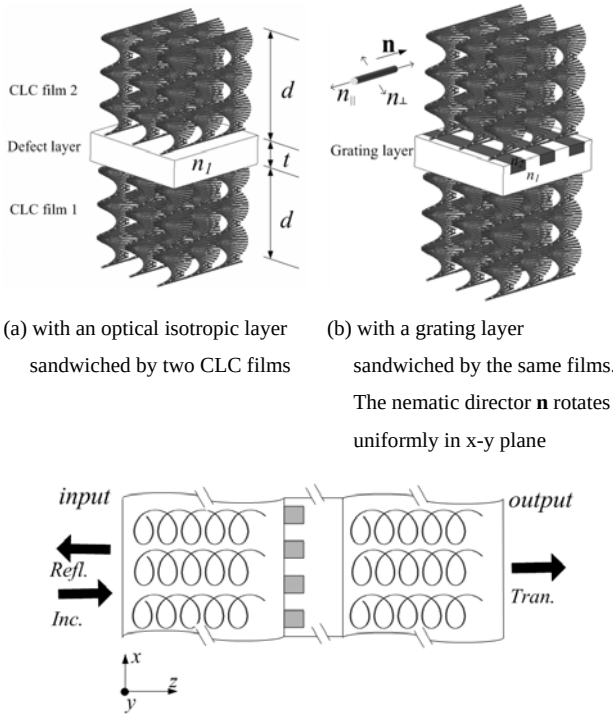

(a) with an optical isotropic layer sandwiched by two CLC films

(b) with a grating layer sandwiched by the same films. The nematic director **n** rotates uniformly in x-y plane

(c) The model system for the 3D FEM simulation. The solid arrows indicate the light propagating directions

(d) Cross section of the rectangular grating

Fig. 1. Schematic drawing of the model system

$$(n_{eff,e}^{(2)})^2 = (n_{eff,e}^{(0)})^2 + (\Lambda/\lambda)^2 \pi^2 f^2 (1-f)^2 (1/n_1^2 - 1/n_2^2)^2 (n_{eff,o}^{(0)})^2 (n_{eff,e}^{(0)})^6 / 3, \tag{2}$$

$$(n_{eff,o}^{(2)})^2 = (n_{eff,o}^{(0)})^2 + (\Lambda/\lambda)^2 \pi^2 f^2 (1-f)^2 (n_1 - n_2)^2 / 3, \tag{3}$$

where the filling factor f is given by $f = a / \Lambda$ (see Fig. 1(d)). $n_{eff,e}^{(0)}$ and $n_{eff,o}^{(0)}$ are the zero-order EMT expression for the effective refractive indices given by

$$(n_{eff,e}^{(0)})^2 = n_1^2 n_2^2 / [(1-f) n_1^2 + f n_2^2)], \tag{4}$$

$$(n_{eff,o}^{(0)})^2 = fn_1^2 + (1-f)n_2^2 . \quad (5)$$

An advantage of the EMT over a rigorous method is that it is less computationally intensive to execute. However, evanescent waves generated by abrupt change in refractive index are not considered in the EMT. The evanescent waves can be reflected by the interface and be coupled into the propagating waves. The effective refractive indices might not be precise to estimate the power transmittance and provide an accurate phase delay produced by the gratings [8, 18]. In rigorous techniques such as finite-difference and finite-element, results are accurate to an arbitrary level of accuracy since no approximations are made to Maxwell's equations and to the theoretical modeling of the configuration itself. For this study, the 3D FEM was chosen as the most developed and suitable modeling approach. For achieving higher accuracy without increasing the number of nodes, Lagrange-quadratic elements are chosen as the basis elements. The discrete model is based on a mesh limit with Δx, Δy, Δz, $\leq \lambda/10$. The absorption by the medium and the surface roughness at the interfaces of the grating layer and the two CLC films are neglected.

III. RESULTS AND DISCUSSION

In the Grandjean structure of conventional CLCs, the central wavelength λ_0 of the stop band in a CLC is given by $\lambda_0 = \bar{n} P_0$, where $\bar{n} = [(n_{||}^2 + n_{\perp}^2)/2]^{1/2}$. The bandwidth is $\Delta\lambda \approx \lambda_o \Delta n / \bar{n} \approx \Delta n P_0$, where $\Delta n = n_{||} - n_{\perp}$ is the birefringence defined by the indices of refraction parallel and perpendicular to the nematic director **n** (as shown in Fig. 1(b)). To verify the accuracy of the 3D FEM model, a simple case is taken to compare their results with those obtained by the transfer matrix method (TMM) [7, 10]. The simulated transmission spectrum using the 3D FEM and Berreman's 4×4 TMM for the normally incident light of right-handed circular polarization (RCP) and left-handed circular polarization (LCP) is shown in Fig. 2 with the case of an isotropic defect layer in the center of the CLC structure (Fig. 1(a), $d = 4P_0$, $n_1 = 1.5$, $t = 750$ nm). The period of the helical twist is $P_0 = 400$ nm. The refractive indices of the birefringent planes in the CLC film are selected to be $n_{||} = 1.7$ and $n_{\perp} = 1.5$. A transmission peak for RCP and a dip for LCP are noted at wavelength of ~641 nm in Fig. 2. The results of a double CLC composite film with a defect layer are shown to have very good agreement with those of the TMM. In addition, the properties of photonic defect modes in CLCs show up in the simulated transmission curves, and the resulting transmission profiles are very similar to Ref. [20].

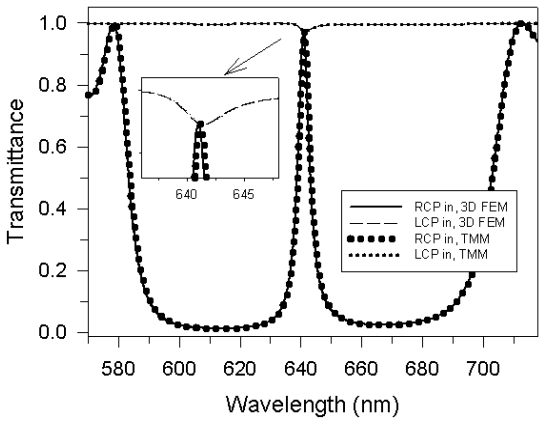

Fig. 2. Comparison of simulated transmission spectrum between the 3D FEM and the 4×4 TMM

The transmission spectrum for the normally incident light of RCP is shown in Fig. 3 with the case of no defect in a CLC structure. The single CLC film thickness is $12P_0$. The stop band is bounded between 600 and 680 nm (shadow: transmittance under 0.05). The other transmission spectrum for incident light of RCP and LCP is also shown in Fig. 3 with the case of a defect layer in the center of the CLC structure (Fig. 1(a), $d = 6P_0$, $t = 750$ nm). A transmission peak for RCP and a dip for LCP related to the localized defect mode are observed at wavelength of ~641 nm.

For normally incident RCP light, Fig. 4 shows the influence of the CLC film thickness in the structure of Fig. 1(a) on the transmittance of the defect mode. By increasing the value of d, a localized state in the transmission spectrum appears, and the peak of the defect mode in the stop band becomes sharper. However, the transmittance of the incident wave at the defect wavelength can exceed 0.5 only when the thickness of both CLC films is under $8P_0$. The incident wave

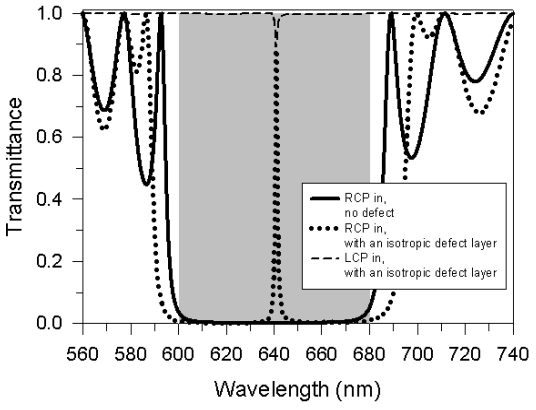

Fig. 3. Transmission spectrum for the structure with no defect/an isotropic defect layer (Fig. 1(a)). The shadow indicates the PBG

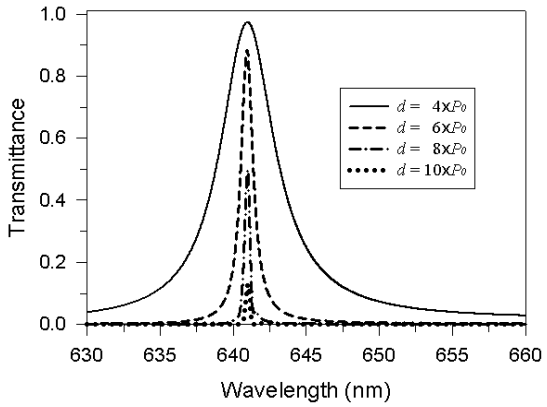

Fig. 4. Transmission spectrum around the defect mode of the structure in Fig. 1(a) for different thickness *d* of the two CLC films

is partly transmitted by the defect structure. One can explain the situation by considering the whole structure as two linked structures, i.e. one is a chiral structure with a defect layer in the middle and the other is a perfect chiral structure. Incident light with wavelength of the defect mode can pass through the defect part, but is partly reflected by the perfect part because its wavelength is in the PBG. Besides, it can be also explained by the anomalous crossover behavior of polarization state in propagation described by Kopp *et al.* [9]. In Figs. 3 and 4, the center wavelength λ_d of the defect mode in the forbidden band is related to the thickness and the refractive index of the isotropic defect layer that satisfy

$$n_1 t = \frac{\lambda_d}{4}(2m+1), \qquad (6)$$

where m=0, 1, 2, …. Eq. (6) can be obtained from thin-film theory [12]. This is the condition for zero reflections at normal incidence through a thin film.

The general behavior of a HSFG appears to be similar to that of optical thin films because only the zeroth diffracted order is allowed to propagate. To prevent other diffracted orders from propagating for normal incidence, the grating period must satisfy Eq. (1). For operation as a form-birefringent zeroth-diffraction-order grating, the grating period of the model shown in Fig. 1(d) is set to be Λ=150 nm, with the filling factor of f = 0.5. Two isotropic materials with refractive indices of n_1=1.5 and n_2=1 (refractive index of air) are used to construct the grating structure. In order to reduce Fresnel reflection, the refractive index of the grating substrate is chosen to be $n_1 = n_\perp$. Therefore, the reduction on the transmittance of a defect mode may be slight. The thickness of both CLC films is d=6P_0. For normally incident RCP light, Fig. 5 shows the transmission spectrum with respect to different normalized groove depth h/Λ of the grating layer. When the groove depth is increased, the position of the defect mode shifts toward smaller wavelength. The reduction in the transmittance of the defect mode is due to light-beam interference in the form birefringence layer. Form birefringence of a HSFG can be characterized by the phase difference between two orthogonally polarized waves propagating through the grating. This anisotropic effect can be used for phase retardation as in retardation plate devices. Controlling the phase delay via the groove depth gives rise to a shift of the resonant mode from the long to the short wavelength.

The center wavelength and the transmittance of the resonant modes are shown in Fig. 6 for normally incident RCP light when the grating grooves of Fig. 1(b) are filled with different refractive index materials. The thickness of the two CLC films is d=6P_0. The normalized groove depth is h/Λ=1. The filling factor is f = 0.5. As the location of the defect mode is shifted by changing the refractive index n_2, there is only one defect state for the range of refractive indices. It is important to note the continuous modulation of the defect mode and the linearity of the sweep in refractive index. This feature can be used to measure the transmission spectra as a function of the refractive index for application of (bio-)chemical sensors and optical refractometers. Even though the transmittance is related to the grating structure, the dominant influence in the transmittance of the defect mode is the sandwiched structure of Fig. 1(a). If the condition satisfies Eq. (6), a maximum transmission will appear at normal incidence. For the case of n_1=1.5 and t=750 nm in Fig. 1(a), the defect wavelength λ_d~643 nm (m=7) will exhibit a minimum reflection. The defect modes near this defect wavelength can obtain higher transmittance as shown in Fig. 6.

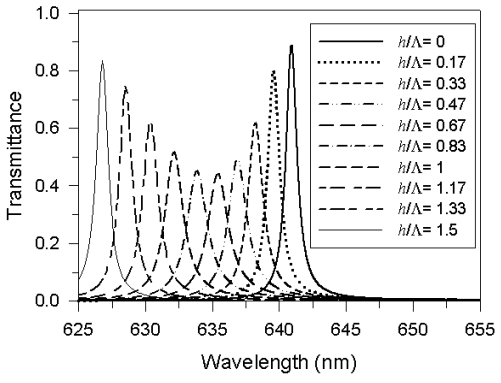

Fig. 5. Transmission spectrum around the defect mode of the structure in Fig. 1(b) for different normalized groove depth *h*/Λ of the grating layer

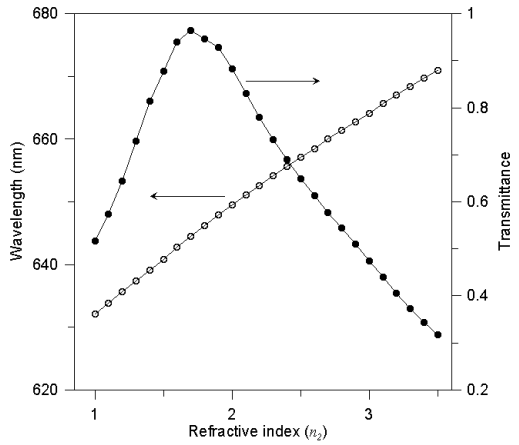

Fig. 6. Center wavelength and transmittance of the defect modes as a function of the refractive index n_2 for the grating grooves filled with different materials

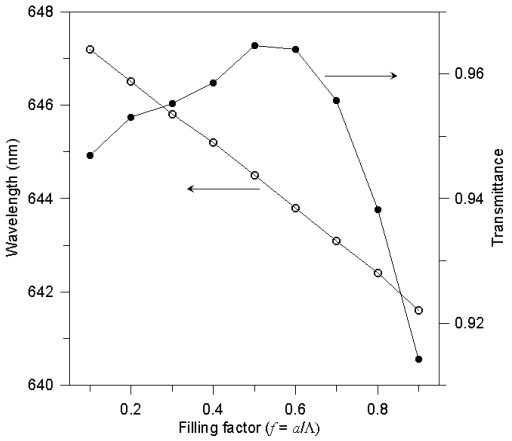

Fig. 7. Center wavelength and transmittance of the defect modes as a function of the filling factor *f*

The center wavelength and the transmittance of the defect modes introduced by the grating as a function of its filling factor are shown in Fig. 7. The thickness of the two CLC films is $d=6P_0$. The normalized groove depth is $h/\Lambda=1$. From Eqs. (2) and (3), form birefringence of a HSFG depends on the filling factor. When the filling factor is increased, the location of the defect wavelength shifts linearly from the long to the short wavelength. It is needed to achieve high transmission for a defect mode with an optimized filling factor. A maximum value of the transmittance for different filling factors is located at $f=0.5$.

IV. CONCLUSIONS

This model system combines the form-birefringence effect of a HSFG with photonic localization in CLCs. The 3D FEM for light propagation in the composite structure is used and compared with Berreman's 4×4 TMM to confirm the accuracy of the model. In the planar cholesteric structure containing a grating layer, the variation of the defect mode via changing grating parameters, such as groove depth, filling factor, and refractive index of the intermixing material, has also been demonstrated for the transmission characteristics. By applying adequate design parameters of groove depth, a higher transmittance can be achieved for a defect mode with a region near the defect wavelength obtained by thin-film theory. The most critical parameter is the refractive index of the dielectric material filled into the grating grooves, which determines a linear sweep in the defect mode. It can be applied as an optical refractometer or a (bio-)chemical sensor, which can be designed by replacing the intermixing material by the medium to be measured.

ACKNOWLEDGEMENTS

The financial supports provided by the Ministry of Economic Affairs under Grant 96-EC-17-A-07-S1-0018 and the National Science Council under Grant NSC 96-2221-E-432-005 are greatly appreciated.

REFERENCES

1. Born, M. and E. Wolf (1980) *Principles of Optics*, 6th ed, Chap. 14. Pergamon Press, Oxford.
2. de Gennes, P. G. and J. Prost (1993) *The Physics of Liquid Crystals*, Clarendon Press, Oxford.
3. Ha, N. Y., Y. Takanishi, K. Ishikawa and H. Takezoe (2007) Simultaneous RGB reflections from single-pitched cholesteric liquid crystal films with Fibonaccian defect. *Optics Express*, 15(3), 1024-1029.
4. Hawkeye, M. M. and M. J. Brett (2006) Narrow bandpass optical filters fabricated with one-dimensionally periodic inhomogeneous thin films. *Journal of Applied Physics*, 100, 044322.
5. Jin, J. (2002) *The Finite Element Method in Electromagnetics*, Wiley, New York, NY.
6. Joannopoulos, J. D., R. D. Meade and J. N. Winn (1995) *Photonic Crystals: Molding the Flow of Light*, Princeton University Press, Princeton, NJ.
7. John, W. D. St., W. J. Fritz, Z. J. Lu and D. K. Yang (1995) Bragg reflection from cholesteric liquid crystals. *Physical Review E*, 51(2), 1191-1198.
8. Kikuta, H., H. Yoshida and K. Iwata (1995) Ability and limitation of effective medium theory for subwavelength gratings. *Optical Review*, 2(2), 92-99.
9. Kopp, V. I. and A. Z. Genack (2003) Twist defect in chiral photonic structures. *Physical Review Letters*, 89(3), 033901.

10. Lakhtakia, A. and R. Messier (2005) *Sculptured Thin Films: Nanoengineered Morphology and Optics*, SPIE Press, Bellingham.
11. Lourtioz, J. M., H. Benisty, V. Berger, J. M Gérard, D. Maystre and A. Tchelnokov (2005) *Photonic Crystals: Towards Nanoscale Photonic Devices*, Springer, Berlin.
12. Macleod, H. A. (1986) *Thin-Film Optical Filters*, Chaps. 1 and 2. Macmillan, New York, NY.
13. Mastui, T., M. Ozaki and K. Yoshino (2004) Tunable photonic defect modes in a cholesteric liquid crystal induced by optical deformation of helix. *Physical Review E*, 69, 061715.
14. Matsuhisa, Y., R. Ozaki, K. Yoshino and M. Ozaki (2006) High *Q* defect mode and laser action in one-dimensional hybrid photonic crystal containing cholesteric liquid crystal. *Applied Physics Letters*, 89, 101109.
15. Matsuhisa, Y., Y. Huang, Y. Zhou, S. T. Wu, R. Ozaki, Y. Takao, A. Fujii and M. Ozaki (2007) Low-threshold and high efficiency lasing upon band-edge excitation in a cholesteric liquid crystal. *Applied Physics Letters*, 90, 091114.
16. Ozaki, M., M. Kasano, D. Ganzke, W. Haase and K. Yoshino (2002) Mirrorless lasing in a dye-doped ferroelectric liquid crystal. *Advanced Materials*, 14(4), 306-309.
17. Ozaki, R., T. Sanda, H. Yoshida, Y. Matsuhisa, M. Ozaki and K. Yoshino (2006) Defect mode in cholesteric liquid crystal consisting of two helicoidal periodicities. *Japanese Journal of Applied Physics*, 45(1B), 493-496.
18. Richter, I., P. C. Sun, F. Xu and Y. Fainman (1995) Design considerations of form birefringent microstructures. *Applied Optics*, 34(14), 2421-2429.
19. Rytov, S. M. (1956) Electromagnetic properties of a finely stratified medium. *Soviet Physic JETP*, 2(3), 466-475.
20. Schmidtke, J. and W. Stille (2003) Photonic defect modes in cholesteric liquid crystal films. *The European Physical Journal E*, 12, 553-564.
21. Song, M. H., B. Park, K. C. Shin, T. Ohta, Y. Tsunoda, H. Hoshi, Y. Takanishi, K. Ishikawa, J. Watanabe, S. Nishimura, T. Toyooka, Z. Zhu, T. M. Swager and H. Takezoe (2004) Effect of phase retardation on defect mode lasing in polymeric cholesteric liquid crystals. *Advanced Materials*, 16(9-10), 779-783.
22. Song, M. H., N. Y. Ha, K. Amemiya, B. Park, Y. Takanishi, K. Ishikawa, J. W. Wu, S. Nishimura, T. Toyooka and H. Takezoe (2006) Defect-mode lasing with lowered threshold in a three-layered hetero-cholesteric liquid-crystal structure. *Advanced Materials*, 18, 193-197.
23. Stork, W., N. Streibl, H. Haidner and P. Kipfer (1991) Artificial distributed-index media fabricated by zero-order gratings. *Optics Letters*, 16(24), 1921-1923.
24. Tyan, R. C., P. C. Sun, A. Scherer and Y. Fainman (1996) Polarizing beam splitter based on the anisotropic spectral reflectivity characteristic of form-birefringent multilayer multilayer gratings. *Optics Letters*, 21(10), 761-763.

Received: Feb. 15, 2008 Revised: Apr. 22, 2008
Accepted: Aug. 07, 2008